Experimental and Theoretical Results on the LAAS Sigma Overbound

Irfan Sayim[*], Boris Pervan[*], Sam Pullen[†] and Per Enge[†]

[*]*Illinois Institute of Technology, Chicago, IL*
[†]*Stanford University, Stanford, CA*

BIOGRAPHY

Irfan Sayim received a B.S. degree from Marmara University (1990), Istanbul, Turkey and ME from Illinois Institute of Technology (1996), in Mechanical and Aerospace Engineering. Currently, he is a Ph.D. candidate at Illinois Institute of Technology and working on Local Area Augmentation of GPS navigation integrity for aircraft precision approach and landing.

Boris Pervan received a B.S. from the University of Notre Dame (1986), M.S. from the California Institute of Technology (1987), and Ph.D. from Stanford University (1996), all in Aerospace Engineering. From 1987 to 1990, he was a Systems Engineer at Hughes Space and Communications Group. Dr. Pervan was a Research Associate at Stanford from 1996 to 1998, serving as project leader for GPS Local Area Augmentation System (LAAS) research and development. He was the 1996 recipient of the RTCA William E. Jackson Award and the 1999 M. Barry Carlton Award from the IEEE Aerospace and Electronic Systems Society. Currently, Dr. Pervan is Assistant Professor of Mechanical and Aerospace Engineering at the Illinois Institute of Technology in Chicago.

ABSTRACT

The Local Area Augmentation System (LAAS) is the differential satellite navigation architecture standard for civil aircraft precision approach and landing. While the system promises great practical benefit, a number of key technical challenges have been encountered in the definition of the architecture. Perhaps chief among these has been the need to ensure compliance with stringent requirements for navigation integrity. In this context, this paper defines a practical way to describe and quantitatively establish LAAS correction error broadcast sigma for final integrity risk assessment at aircraft. The method involves a synthesized solution of both data-based analysis for gaussian (or nearly gaussian) error sources and a theoretical bound for non-gaussian error sources such as ground reflection multipath. In addition, this paper covers the largely unresolved issues (binning, etc.) concerning sigma quantification by direct use of data.

INTRODUCTION

Local Area Augmentation System (LAAS) integrity risk is quantified at the aircraft via the computation of Vertical and Lateral Protection Levels (termed VPL and LPL, respectively). The prescribed algorithms for the generation of these protection levels implicitly assume zero-mean, normally distributed fault-free error distributions for the broadcast pseudorange corrections. While the assumed error model may be consistent with the effects of thermal noise and diffuse multipath, it is understood that remaining errors such as ground reflection multipath and systematic reference receiver/antenna errors are not necessarily reliably modeled by zero-mean normal distributions. Therefore, to ensure that the computed values of VPL and LPL at the aircraft are meaningful and that integrity risk is properly managed, special care must be taken by the LAAS Ground Facility (LGF) in the establishment of the broadcast pseudorange correction error standard deviation (σ_{pr_gnd}). In this paper, we address major remaining unresolved issues concerning the establishment of σ_{pr_gnd}. These include the definition of a sufficient process by which empirical error data may be processed to ensure spatially stationarity of error, quantification and compensation for the effects of seasonal variation of error, and a methodology to account for potential non-Gaussian error sources.

For normally distributed errors such as receiver thermal noise and diffuse multipath, standard deviations can be estimated using experimental data alone. In this case, however, it is still necessary to account for the additional integrity risk incurred by statistical uncertainty (due to finite sample size) in the knowledge of reference receiver

error standard deviation and error correlation between multiple reference receivers. In this regard, a detailed methodology has been developed for the definition of minimum acceptable inflation parameters for the sample standard deviation [1]. (The inflation parameters are functions of the number of samples available and the sample correlation coefficient.) However, in order for such an empirical process to be applied, it is first necessary to define a proper method to collect data into spatial bins prior to sigma estimation. While large bin sizes are desired to maximize sample size (to limit required inflation factors), bin size is ultimately constrained by the need for spatial stationarity of all data within the bin (i.e., all error data within a bin must have the same underlying distribution). The quantitative resolution of this critical tradeoff, which is conceptually illustrated in **Figure-1**, is a major subject of the work described in this paper.

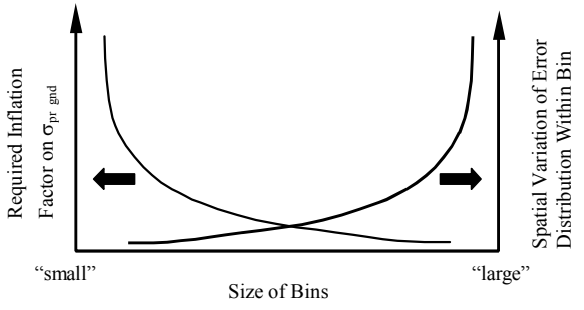

Figure-1 Sketch of Error Variation within Bins

The effects of seasonal variations in pseudorange correction error (in particular multipath) must also be accounted for in the broadcast σ_{pr_gnd}. However, it is clearly impractical to collect a full-year span of data (prior to commissioning) for each LGF to account for such effects. Therefore, archived error data collected at the LAAS Test Prototype (LTP) facility at the W. J. Hughes FAA Technical Center is used to define a baseline LGF model for seasonal variation in σ_{pr_gnd}. The observed LTP temporal variation is used to define a common standard inflation factor for use in the establishment of σ_{pr_gnd} in future LGF installations until sufficient site-specific data is collected.

Because ground multipath error is not necessarily normally distributed, empirically computed (and inflated) values of σ_{pr_gnd} are not sufficient to guarantee overbounding of the total LGF ranging error. Furthermore, it is impossible to rely on empirically constructed distributions (e.g., error data histograms) alone to define the nature of the underlying error distribution because little or no empirical data will exist in the 'tails' (which are of greatest interest in LAAS). Therefore, theoretical approaches are emphasized in our work to incorporate ground reflection multipath effects into σ_{pr_gnd}.

The ultimate goal of this work is to define a sufficient methodology for the establishment of the LAAS broadcast σ_{pr_gnd}. Neither theoretical approaches nor empirical error data alone are adequate in this regard. The final broadcast pseudorange sigma will be a result of both elements. In this paper, we introduce a practical way to synthesize the empirical and theoretical elements to quantitatively establish σ_{pr_gnd} for LAAS.

RANGING ERROR CHARACTERISTICS

In general, the pseudorange error has three important characteristics. These are:

I -Repeatability
II -Serial Correlation
III -Nonstationarity

A simple illustration of data showing these characteristics is sketched in **Figure-2**. In this paper, we emphasize the quantification and accommodation of these characteristics in LAAS broadcast sigma establishment rather than their causes and mitigation.

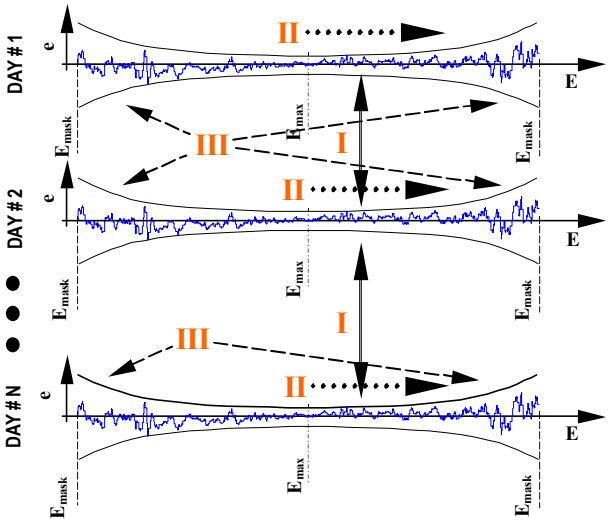

Figure-2 Sketch of Error Characteristics

I- Repeatability (Day-to-Day Correlation): It is well known that the ranging error, in general, is repeatable (or correlated) day-to-day. The repeatability characteristic is mainly caused by multipath error and it can be easily observed with a stationary (fixed) antenna when the environmental conditions are constant.

Because of the repeatability property, calibration of error is possible in principle. For example, use of a prior days error data to correct errors on the current day may reduce ranging error size. However, the fundamental problem regarding statistical description of the (residual) error distribution and sigma bounding remains unsolved.

Another ramification of error reparability is that sigma cannot be easily established by ensemble of data over many days. There are two basic reasons for this: 1) data ensembled over many days will exhibit significant correlation effects between days (i.e., samples are not independent), 2) the sigma establishment process must be reasonably short for practical LGF initialization.

Therefore, the approach taken in this work is to generate sigma from data collected over a single (commissioning) day and then inflate the result to account for long-term seasonal variation of the error observed at the LTP site (where several years worth of archived data are available).

II- Serial Correlation: One of the most significant characteristics of the observed ranging error is serial correlation between recorded samples of data. This correlation effectively limits the number of independent samples that can be assumed in the calculation of inflation factors that account for statistical uncertainty in the estimated sigma. In general, the number of independent samples for computing inflation factor will be a function of the size of the bin and the correlation time of the data within it.

III- Nonstationarity: A nonstationary process is defined as process in which statistical parameters of distribution do not stay constant in time. Elevation dependency of multipath delay and GPS antenna gain patterns are a common source of nonstationarity in observed ranging error. With the MLA antennas used for LAAS, these effects are reduced, but they are still present and significant near the cut-off angle between the MLA and the HZA (High Zenith Antenna). In addition, nonstationarity may also exist due to azimuthal variations (e.g., discrete reflectors or diffractors) in the antenna.

EXPANDING BIN (EB) CONCEPT

The Expanding Bin (**EB)** method is a new approach for data-based sigma establishment that simultaneously manages the effects of nonstationarity and serial correlation of observed error data. Traditional approaches toward data-based sigma establishment rely on fixed bin widths, which are selected a priori with intent to both minimize the effect of mixing of error data derived from distributions and maximize the number of samples within each bin. In practice, the appropriateness of prior bin size selection is difficult to quantitatively validate and is therefore often judged via ad hoc inspection of the data. In contrast, the **EB** method is an *adaptive* scheme which automatically selects the bin width at a given time (or elevation) for each satellite separately. In practice, the result is achieved by considering not only a single bin width but all possible bin widths at the given time/elevation. The inherent tradeoff in bin size selection resulting from the simultaneous presence of nonstationary and serial correlation is gracefully controlled by *selecting the worst-case inflated sigma* as representative of given time/elevation (**E**).

The **EB** method is implemented separately for each satellite by the following means: First, a core bin **BI** is defined to provide a minimum allowable independent sample size for sigma estimation. This is performed by using the entire data set from the satellite pass to compute the error correlation time, which is in turn translated into the time between independent samples. With this result the core bin size BI is set. Second, a maximum-size bin **BM** is defined in order to provide a wide range for estimating many candidate sigmas. In principle, **BM** can be selected to include the entire data set. A simple sketch of inner (core) and outer bins, **BI** and **BM** respectively, is shown in **Figure-3** for an arbitrary time/elevation **E**.

The mathematical description of the process for a representative sigma at time/elevation **E** can be expressed as:

$$\sigma_E = \max_j \{\sigma_{E,j}\} \qquad (1)$$

where, **j** is the bin width index ranging from **BI** to **BM** .

After sigma is selected for a given time/elevation using equation (1), the entire process repeated at next data epoch until the end of the data set is reached.

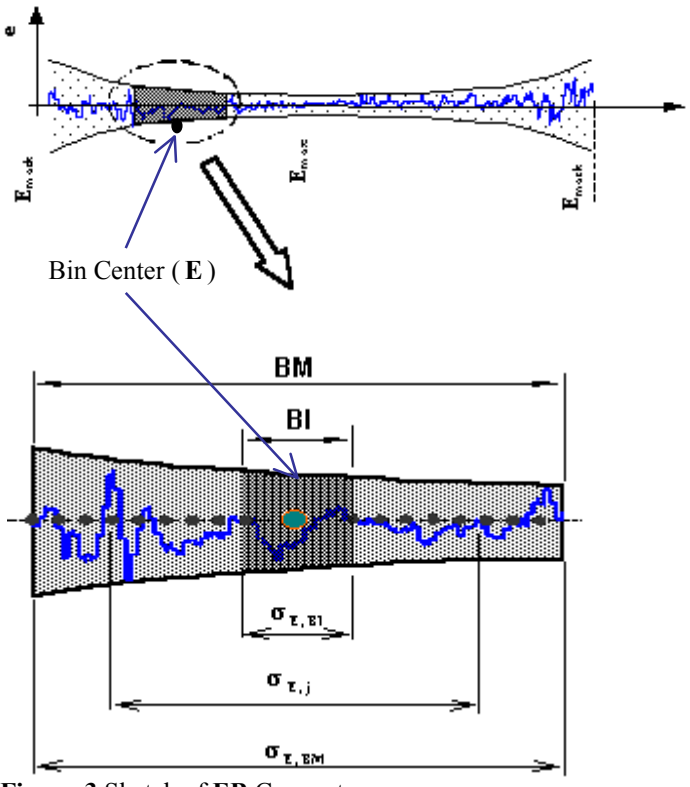

Figure-3 Sketch of **EB** Concept

COMPUTATION OF SIGMA

Given the conceptual introduction of **EB** method in previous section, the mechanization of the process can now be described in greater detail. To aid in this description, a flow chart of sigma computation process is shown in Figure 4.

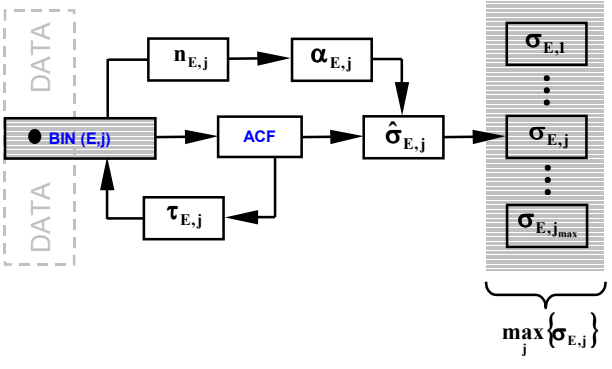

Figure-4 Flow Chart for Sigma Computation

As illustrated previously (**Figure-3**), the computation starts from a predefined range of data sized with **BI** and follows by continuously adding new measurements in both time directions of it. Each new increased data set is passed through the computation algorithm shown in the flow chart of **Figure-4**. First the sample autocorrelation function (ACF) for the selected data set is computed, and a resulting correlation time estimate is extracted from the ACF by assuming a first order Gauss-Markov process [5]. Simultaneously, the sample variances are computed from the selected data set. The number of independent samples in the binned data is computed by simply dividing the number of recorded samples in the selected data set by twice the estimated correlation time.

Based on the number of available independent samples, an inflation factor is generated to account for statistical uncertainty the computed sample standard deviation. The details of the computation of these inflation factors from an integrity risk perspective are provided in reference [1]. In this paper, however, inflation factors are directly generated by the use of a 99.9% confidence interval. The associated in factor is plotted as a function of the number of independent samples in **Figure-5**. It is clear that a small number of independent samples requires high inflation factor on sigma to cover estimation uncertainty.

For each bin size, the computed sample standard deviation is inflated and the result is stored. When all candidate bin sizes are processed, the upper bound inflated sigma is selected as follows:

$$\sigma^{s}_{m,E} = \max_{j}\left\{\sigma_{m,E,j}\right\} = \max_{j}\left\{\alpha_{m,E}(n_{m,E,j})\hat{\sigma}_{m,E,j}\right\} \qquad (2)$$

where $\alpha_{m,E}(n_{m,E,j})$ is the inflation factor given that $n_{m,E,j}$ independent samples are available for reference receiver **m**, time epoch **E**, and bin width index **j**; $\hat{\sigma}_{E,j}$ is the computed standard deviation of data at epoch **E** and bin width index **j**.

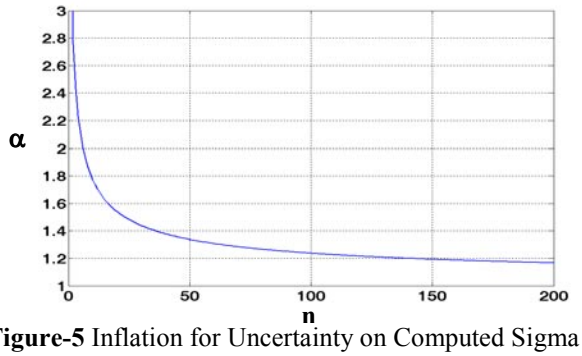

Figure-5 Inflation for Uncertainty on Computed Sigma as a Function of Independent Sample Sizes

BENCHMARK TEST OF EB METHOD

Two sigma results, obtained by two different methods, are shown in **Figure-6**: 1) the sigma history generated by the **EB** method, and 2) the inflated sigma generated by use of

entire data set. It can be observed, by visual inspection of **Figure-6**, that the **EB**-generated sigma appears to be a faithful representation of the variation of the error data itself (which is also shown on the plot), because sigma vs. time profile is shaped not only by slow variation of error (serial correlation effect) but also by the size of sample standard deviation (nonstationarity) of error data.

The flat line is the sigma obtained by use of entire data. This sigma indicates that if we mix all the error distributions within a single bin (without regard to nonstationarity effects) the sigma will not represent error variation properly.

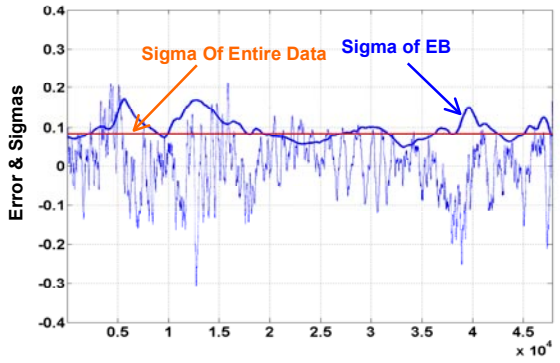

Figure-6 Sigma Generation for Nonstationary Process

Comparisons of two sigmas in CDF (Cumulative Distribution Function) sense are shown in **Figure-7**. In this figure, the performance of both methods is compared against a standard normal distribution by normalizing the actual error data by each of the two sigma curves and then plotting their corresponding CDFs.

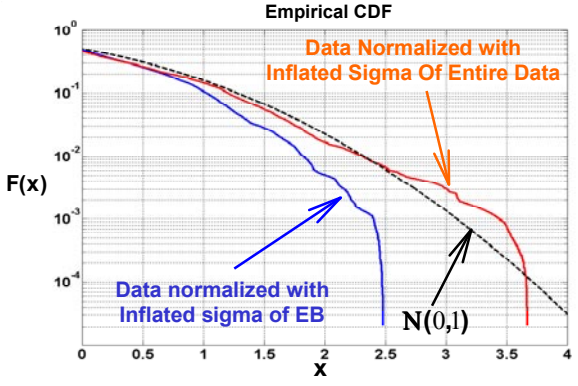

Figure-7 Performance Comparison of New Method

It is clear from the figure that for the **EB**-normalized case a significant margin exists with respect to an overbounding standard normal distribution. In contrast, the standard normal distribution is insufficient to overbound the error data normalized by the inflated sigma of the entire data set. The basic reason for this fact is that the latter approach does not account for nonstationarity (i.e., mixing of data from different error distributions during the satellite pass).

CORRELATION BETWEEN RECEIVERS

In the LAAS VPL computations, it is implicitly assumed that ranging errors are uncorrelated across ground receivers. In fact, the existence of any such correlation is not strictly consistent with the VPL equations since the σ_{pr_gnd} for an individual reference receiver is always divided by the number of receivers to account for the averaging of uncorrelated receiver measurements. In reality, however, it is possible that some measurable correlation exists. Furthermore, even if a negligibly small correlation coefficient is computed from a finite sample set, the statistical uncertainty in the estimate must also be accounted for. Such uncertainty is lessened, as one would naturally expect, as the sample size used to estimate correlation coefficient increases.

To accommodate the effects of correlation, we assume that the ground error standard deviation for any given reference receiver is expressed by equation (2). The effect of correlation between receivers when averaging $\mathbf{M}$ reference receiver errors can be modeled as an effective increase in $\sigma^{s}_{m,E}$ as follows:

$$\sigma^{sc}_{m,E} = \beta_m \sigma^{s}_{m,E} \tag{3}$$

where,

$$\beta_m = \begin{cases} \sqrt{1 + \sum_{\substack{i=1 \\ i \neq m}}^{M} \rho_{mi}} & \rho^{+}_{m} \geq \rho^{-}_{m} \\ 1 & \rho^{+}_{m} < \rho^{-}_{m} \end{cases} \tag{4}$$

where the total positive correlation between receivers is defined by, $\rho^{+}_{m} = \sum_{\substack{i=1 \\ i \neq m}}^{M} (\rho_{mi} \geq 0)$, and the total negative correlation by $\rho^{-}_{m} = \left| \sum_{\substack{i=1 \\ i \neq m}}^{M} (\rho_{mi} < 0) \right|$.

Note that any inflation of sigma due to negative correlation is irrelevant since the initial (implicit)

assumption of uncorrelated receiver errors will already result in over inflation in this case.

The statistical relationship between measured (sample) correlation ($\mathbf{r}$) and the true correlation coefficient correlation ($\boldsymbol{\rho}$) is given in [3]:

$$\frac{1}{2}\ln\left(\frac{1+r}{1-r}\right) \sim N\left(\frac{1}{2}\ln\left(\frac{1+\rho}{1-\rho}\right), \frac{1}{\sqrt{n-3}}\right) \quad (5)$$

where $\mathbf{n}$ is number of independent samples used to compute $\mathbf{r}$. The 99.9% confidence contours for $\boldsymbol{\rho}$ are plotted in **Figure-8** versus $\mathbf{r}$ and $\mathbf{n}$.

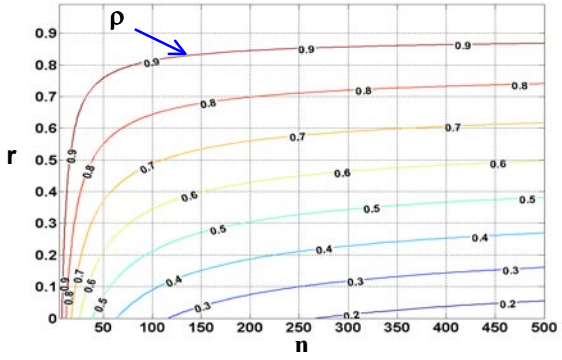

Figure-8 Contours of 99.9% Confidence Correlation as a Function of Measured Correlation and Independent Samples

TEMPORAL VARIATION OF ERROR

In this section, the process of quantification and accommodation of temporal variation is detailed using a representative example. The procedure is based on the relative maximum variation between average sigmas across seasons. The goal, as mentioned earlier, is to establish sigma from a limited duration of LGF commissioning data (one day) and scale by a factor (γ_m), derived from long-term archived LTP data, to account for temporal variation:

$$\sigma_{m,E}^{sct} = \gamma_m \sigma_E^{sc} \quad (6)$$

The long-term temporal variation factor (γ_m) is obtained using a one-year span of LTP data, with four seasonal samplings of two weeks per season,. Each day of archived LTP data consists of error measurements from three LAAS Integrated Multipath Limiting Antennas. A satellite (PRN#2, arbitrarily chosen in this example), for which we previously established sigma values using the **EB** method on the initial day's worth of data, is used to generate temporal variation effects. All of the ranging errors on the subsequent days of data for this satellite are first normalized by initial day's **EB** sigma values. (This is done so that the temporal variation relative to the initial day's **EB** result can be directly observed.) Then the standard deviations of each normalized error data set computed. The normalized error standard deviations are then grouped into four averaged seasonal samplings. The reason for seasonal grouping and averaging sigmas seasonally is that we are interested in characterizing the effects of long-term, slowly-varying effects due to the weather-related environmental changes. Finally, the average standard deviation of each season is sorted from minimum to maximum, and the ratio between maximum and minimum average sigma is selected as temporal variation scale factor (γ_m) as shown:

$$\gamma_m = \frac{\max(\sigma_{m,seasons})}{\min(\sigma_{m,seasons})}, \quad (7)$$

where,

$\sigma_{m,seasons} = \left[\bar{\sigma}_{m,winter} \quad \bar{\sigma}_{m,spring} \quad \bar{\sigma}_{m,fall} \quad \bar{\sigma}_{m,summer}\right]$, and $\bar{\sigma}_{m,winter}$, $\bar{\sigma}_{m,spring}$, $\bar{\sigma}_{m,fall}$, and $\bar{\sigma}_{m,summer}$ are averages of normalized error standard deviation for the winter, spring, fall, and summer seasons, respectively.

The seasonal variation inflation factor result for the particular satellite considered here (PRN#2) is $\gamma_1 = 1.1362$.

It is important to note that in this work only a single satellite/single receiver case is considered so far. A more detailed analysis (for multiple satellites and receivers) must be conducted to define a generalized seasonal variation inflation factor suitable for use in the LGF sigma establishment process.

GROUND REFLECTION MULTIPATH

Due to the slowly-varying nature of ground-reflection multipath, it is unlikely that its effect on sigma can be quantified by experimental means alone. Therefore, in past work [5], a number of candidate theoretical approaches were defined for the establishment and inflation of sigma in this regard. A relatively conservative example model, **Uniformly Distributed Relative Phase and Constant Reflection Strength,** is selected from these candidates as a representative example. For this model, it is shown in reference [5] that ground reflection multipath can be bounded by a zero mean gaussian distribution with standard deviation

$$\sigma_{MP} \geq 1.05(D/U)\min[2h\sin E, d] \quad (8)$$

Where, **D / U** is the amplitude of reflected signal relative to direct, **h** is antenna height, **E** is elevation angle, **d** is the half correlator spacing (e.g., 0.05 chip = 15m).
In **Figure-9**, this example model, equation (8), is plotted in the lower trace by using the values of relative signal strength [6] given in the upper plot and LTP receiver characteristics.

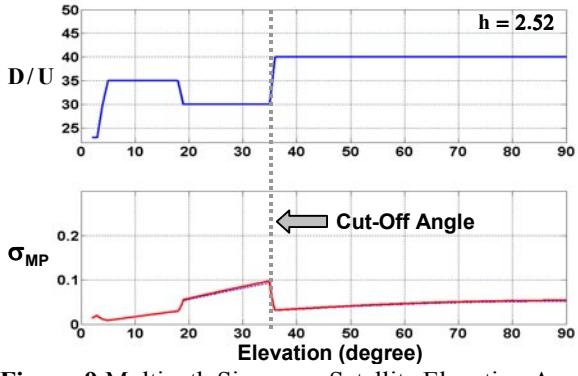

Figure-9 Multipath Sigma vs. Satellite Elevation Angle

While the ground reflection multipath resulting from the selected model is not gaussian, it is shown in reference [5] that if the bounding value of multipath sigma in equation (8) is combined via root-sum-square with sigmas from other gaussian error sources, gaussian overbounding is preserved. This is an important issue relevant to the sigma synthesis discussion given in the next section.

SYNTHESIS OF BROADCAST SIGMA

To accommodate all contributing, independent error sources, establishment of broadcast sigma must include:

1-Sigma Estimated From Data: To accommodate gaussian (or nearly gaussian) error sources,

- A very limited (one day) data analysis must be done for every new installation and sigma must include:
  - Inflation due to sample standard deviation uncertainties (α)
  - Accommodate the effects of nonstationarity ('mixing') of error data within bins.
  - Inflation due to correlation between receivers (β).
- Seasonal Data Analysis:
  - Inflation due to long-term temporal variation (γ).

2-Theory/Analysis: To accommodate multipath (non-gaussian) error sources,

- A theoretical model must be defined (e.g., ground reflection multipath models from reference [5]) and combined (RSS) with estimated sigma from data.

Because neither theoretical approaches nor empirical error data alone are adequate, the final broadcast pseudorange sigma will be a result of both elements. The candidate sigma establishment process is defined here:

1- Use the **EB** method to generate the maximum obtainable sigma values from data. (The **EB** approach implicitly incorporates nonstationarity effects and inflation for sample standard deviation estimation uncertainty.)

$$\sigma^{s}_{m,E} = \max_{j}\left\{\sigma_{m,E,j}\right\} = \max_{j}\left\{\alpha_{m,E}(n_{m,E,j})\hat{\sigma}_{m,E,j}\right\} \qquad (9)$$

2-Account for correlation effects between reference receivers,

$$\sigma^{sc}_{m,E} = \beta_{m}\sigma^{s}_{m,E} \qquad (10)$$

3-Account for long-term temporal (seasonal) error variation,

$$\sigma^{sct}_{m,E} = \gamma_{m}\sigma^{sc}_{E} \qquad (11)$$

4- Generate the composite sigma from data,

$$\sigma^{comp}_{M,E} = \sqrt{\frac{\sum_{m=1}^{M}\left(\sigma^{sct}_{m,E}\right)^2}{M}} \qquad (12)$$

5-Combine with the theoretical multipath sigma bound,

$$\sigma_{pr\_gnd} = \sqrt{\left(\sigma^{comp}_{M,E}\right)^2 + \sigma^2_{MP}} \qquad (13)$$

AN ILLUSTRATIVE EXAMPLE RESULT

The following data specifications are used in the example analysis that follows:

Site: FAATC/LAAS Test Prototype
BI: 1000 Recorded Samples
BM: 5000 Recorded Samples
Conf. Interval for Inflations: 99.9%
Number of Reference Receivers: 3
Satellite: PRN#2
Elevation Mask: 5 degree
Cut-Off Angle of MLA: 35 deg
C/N_O Mask: 40 dB-Hz.
Smoothing Time Constant: 100 sec.
Raw Data Sample Rate: 2 Hz
Time of Data Record: February 2000

First, sigmas are estimated by direct use of data with the **EB** method. Each sigma trace is then plotted (solid

curve) in **Figure-10** for RR1 (reference receiver #1), RR2, and RR3, from top to bottom respectively. For comparison, the actual error data is also plotted. It is observed that the sigma traces for RR1 and RR2 are generally larger than that for RR3. We should also note that the worst sigma values are obtained near by the cut-off angles (vertical dashed lines) of HZA and also that a significant contribution of HZA error to MLA (Dipole) sigma is clearly observed.

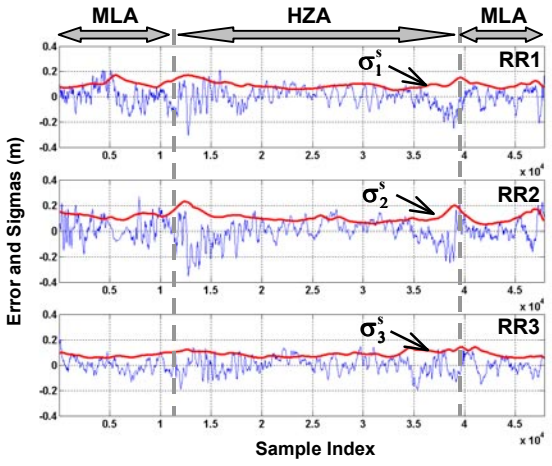

Figure-10 Sigma of **EB** Method for each RR

The sigmas traces of **Figure-10** are plotted in the upper plot of **Figure-11** for more direct comparison of relative performance between reference receivers. The bottom plot within the figure shows the composite (average) sigma of three RRs. The composite broadcast sigma of three-reference receivers is about 10 cm except near cut-off angle regions.

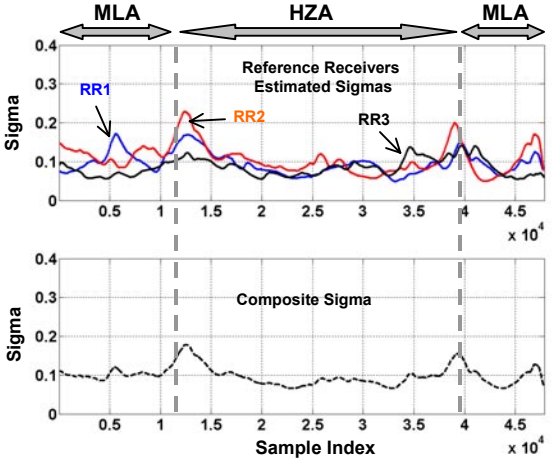

Figure-11 EB Sigmas (Individual and Composite)

The **EB**-sigma-normalized error distributions (CDFs) for the three receivers are plotted in **Figure-12**. It is clear that each reference receiver's normalized error is conservatively overbounded by a standard normal CDF.

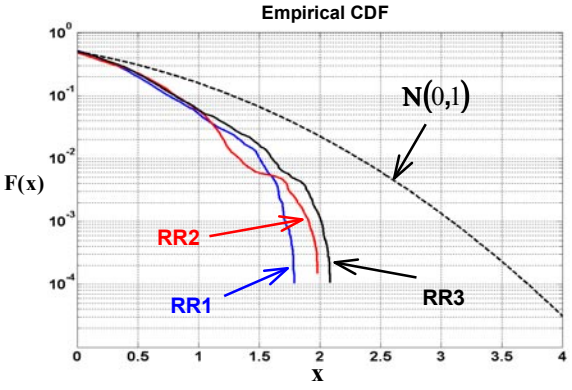

Figure-12 CDF Overbound of **EB** sigmas

Correlation effects between receivers are applied to sigmas of **EB** and then plotted in **Figure-13**. For this example, the composite sigma of three reference receivers is inflated as a function of the number independent sample within the data, as defined in equation (4). The upper curve shows composite sigma that is generated after each reference receiver's sigma is independently inflated for correlation using the values listed in **Table-1**.

r / ρ	m = 1	m = 2	m = 3	β
m = 1	1	0.21/0.38	0.19/0.37	1.3264
m = 2	0.21/0.38	1	0.03/0.22	1.2711
m = 3	0.19/0.37	0.03/0.22	1	1.2638

Table-1 Correlation Values

In **Table-1**, the measured (**r**) and 99.9% confidence (**ρ**) values of correlation between reference receivers are given. These values are converted to correlation inflation factors (**β**) listed in the last column.

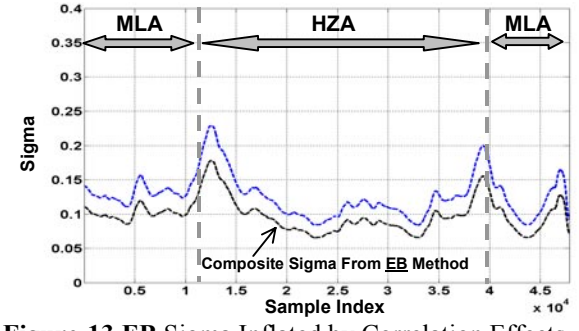

Figure-13 EB Sigma Inflated by Correlation Effects

In the **Figure-14**, the effect of temporal variation is applied to sigma (after correlation effects have been applied). For the time being, we have available only the

temporal variation inflation factor result for RR1. Therefore, we assume that the temporal inflation factors for the other two receivers are the same ($\gamma_1 = \gamma_2 = \gamma_3 = 1.1362$). The upper curve is the final sigma trace obtained from data-based estimation.

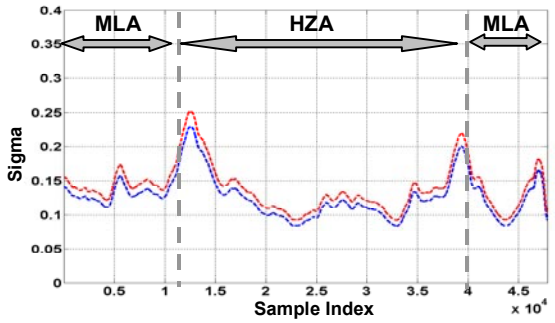

Figure-14 Data Based Sigma (Sigma of **EB** Inflated by Correlation and Temporal Variation Effects)

In **Figure-15**, the overbounding ground reflection multipath sigma, plotted in **Figure-9**, is combined with data-based sigma of **Figure-14**.

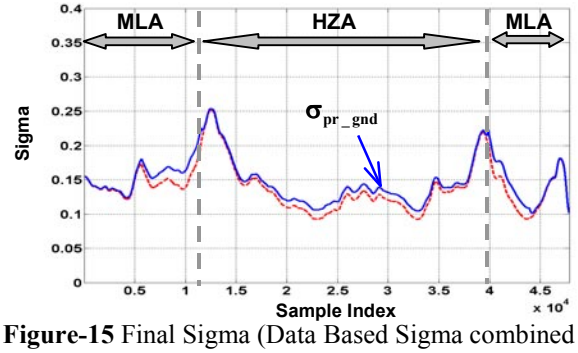

Figure-15 Final Sigma (Data Based Sigma combined with Multipath Sigma)

The final composite broadcast sigma result, σ_{pr_gnd}, is plotted in **Figure-16** and compared with LGF **C3** and **B3** broadcast sigma specifications [2].

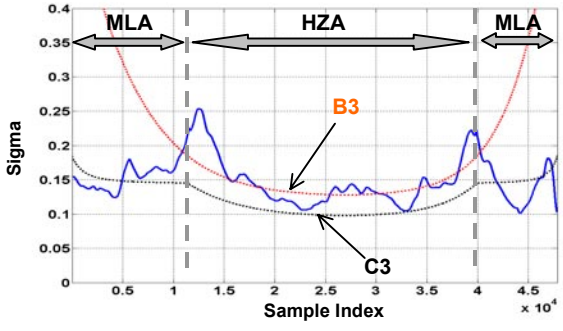

Figure-16 Final Sigma Result vs. Specifications

In this example, it is clear that established σ_{pr_gnd} exceeds **C3** and **B3** specifications. However, it is possible that σ_{pr_gnd} may be reduced by one or more of the following means:

1. Refined calibration of code-carrier phase center offsets for the LGF data used in this work.

2. Cut-off angle (transition angle between HZA and Dipole) can be varied to some degree to reduce sigma peaks.

3. The sigma performance of one or two receivers may be acceptable without the aid of the remaining receivers, which may have higher sigmas. (For this example, RR3 has significantly lower error than the other two receivers near the peaks at 35 deg). Therefore, RR masking at certain elevations where sigma is large may prevent unacceptable composite sigma results.

4. It may be possible to use smaller inflation factors based on the entire data set, given that data normalized by **EB** sigmas is overbounded by standard normal CDF.

An example of the application of item 4 is discussed in more detail below. The approach is motivated by the observed result that error data normalized by EB-sigmas which are *not* inflated for statistical uncertainty are nevertheless still overbounded by a standard normal distribution.

In **Figure-17**, the previous final sigma results are modified by scaling *uninflated* **EB**-sigmas by the (statistical uncertainty) inflation factor derived from the number of independent samples within the entire set (satellite pass) of data. Sigma for this case is defined as

$$\sigma^{s}_{m,E} = \alpha_{m,all}(n_{m,all}) \max_{j} \left\{ \hat{\sigma}_{m,E,j} \right\} \qquad (14)$$

where $\alpha_m(n_{s,all})$ is the inflation factor given that independent sample size $n_{m,all}$ is available for a bin width corresponding to the entire data set. Obviously, the entire data set has more independent samples than any subset bins, so the effect of inflation due to statistical uncertainty will be much smaller in this case. Therefore, the final sigma results will be reduced even if the other effects (correlation and temporal variation) remain unchanged. It is clear that the new results are significantly improved such that the **C3** specification is nearly satisfied, with exceptions at the sigma peaks near the cut-off angle regions. However, because the impetus for this modified approach to inflation is derived primarily from empirical

observations, rather than from theoretical arguments, additional work is required to validate the applicability of these results.

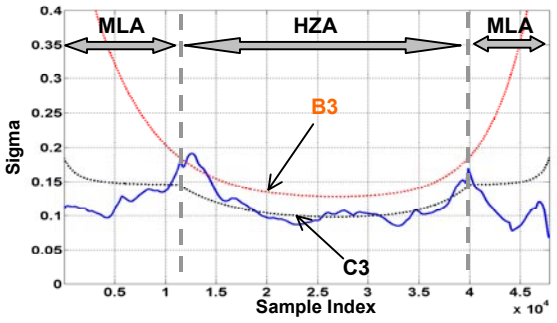

Figure-17 Final Sigma Result vs. Specifications

CONCLUSIONS

In this paper, a new adaptive bin selection approach, known as the Expanding Bin (**EB)** Method, is defined and applied to nonstationary and autocorrelated ranging error data is proposed for establishment of LGF broadcast sigma. The results in this paper show that:

- Using the **EB** method, the upper-bound sigma trace (as a function of time/elevation during the satellite pass) is directly extracted from the available data.
- The **EB**-method implicitly accounts for nonstationarity and inflation for statistical uncertainty.
- Error data normalized by **EB**-sigmas are conservatively overbounded by a standard normal CDF.
- Abrupt variations in sigma across bin boundaries, which exist in the fixed-bin approaches, are naturally eliminated using the **EB** approach.

An analysis of long-term (seasonal) error variation is performed. The maximum, relative, normalized temporal variation observed using archived LTP data was selected as a sigma scale factor. The approach is suggested for use as a baseline for other LGF sites until they have collected sufficient data.

In addition, the effects of correlation between receivers and prior theoretical results for (non-gaussian) ground reflection multipath errors are directly addressed. Finally, a detailed candidate methodology for LGF sigma establishment is proposed in this paper.

ACKNOWLEDGEMENTS

At the FAA Technical Center, the assistance and constructive comments of John Warburton is greatly appreciated. The authors gratefully acknowledge the Federal Aviation Administration for supporting this research. However, the views expressed in this paper belong to the authors alone and do not necessarily represent the position of any other organization or person.

REFERENCES

[1] B. Pervan, and I. Sayim, "Sigma Inflation for the Local Area Augmentation of GPS," *IEEE Transactions on Aerospace and Electronic Systems*, Volume 37, Number 4, October 2001

[2] RTCA (SC-159/WG-4), "Minimum Aviation System Performance Standards for the Local Area Augmentation System (LAAS)," RTCA/DO-245, RTCA Inc., Washington DC, 28 September 1998.

[3] Julius S. Bendat and Allan G. Piersol, "Random Data, Analysis and Measurement Procedure," 2nd, Edition, John Willey & Sons, 1986

[4] Arthur Gelb, "Applied Optimal Estimation," The M.I.T. Press, 1999

[5] B. Pervan, S. Pullen, and I. Sayim, "Sigma Estimation, Inflation and Monitoring in the LAAS Ground System," *Proceedings of the 13th International Meeting of the Satellite Division of the Institute of Navigation (ION GPS-2000)*, Salt Lake City, UT, September 2000

[6] R. Braff, "Description of the FAA's Local Area Augmentation System (LAAS)," *Journal of the Institute of Navigation*, Vol. 44, No. 4, winter 1997-1998